

IMPLEMENTATION OF THE DYNAMIC BALANCING APPROACH OF A ROTATING COMPOSITE HOLLOW SHAFT

Ala'a M. Al-Falahat

Department of Mechanical Engineering

Mutah University

Mutah, Al-Karak, Jordan, 61710

alaa.falahat@mutah.edu.jo

Abstract

Balancing is essential in rotating machinery, which is widely employed in many technical sectors, particularly in high-speed rotor-bearing systems. The mass balancing method of the hollow shaft manufactured of composite materials is investigated in this study over the whole speed range of the rotor. The main goal of the balancing technique is to generate a smooth-running machine by removing the commonality imbalance mass through the use of compensating mass unbalance. As a result, MATLAB code is created to produce a functioning mathematical model of the rotor-bearing system. The unbalanced rotor-bearing system finite element model is proposed to set the balancing mass of the composite hollow shaft at a selected speed rotor that allows minimizing the vibration response amplitude of the rotor as much as possible with minimal impact on the rest of the imbalance response within the speed range of the interest. As a consequence, this study validates the process for distributing imbalance in modelling balancing to balance the flexible hollow shaft with an unbalanced mass throughout the complete speed range of the shaft. The balance of the hollow shaft at the critical speed was observed in this approach, and the vibration amplitude was determined by adding extra mass at a specific angle.

Keywords: composite hollow shaft, balancing, mathematical modelling approach, critical speed.

DOI: 10.21303/2461-4262.2022.002336

1. Introduction

Rotor mass imbalance is a typical problem in rotating machinery, which is widely employed in a range of technical sectors [1–3] such as vehicles, aircraft gas turbine engines, electrical motors, and power generation. The imbalance term indicates the deviation and imperfections of the mass centre from the rotation axis [4]. As a result, balancing the vibrating rotor system due to imbalanced force is critical to minimize unwanted vibration and improve dependability, because vibration induced by unbalancing may damage major machine elements such as bearings, gears, and couplings [5].

The hollow shaft rotor mass balancing method is used in this study, and the main goal of the balancing procedure is to produce a smooth operation machine by attempting to eliminate commonality unbalance mass or by applying compensating mass unbalance. However, because the unbalanced mass is dispersed over the length of the rotor, total elimination of the mass imbalance is usually impossible and unneeded [6].

A hollow shaft made of composite material is selected because it has valuable properties such as higher strength and stiffness, as well as the ability to outperform the same loads with less weight when compared to solid material made of metals, so it is better to choose for the load-bearing type [7].

The mathematical technique has been applied and developed in several types of research [8, 9]. Finite element simulation is considered a potential method for analyzing engineering applications such as rotor dynamics in rotation systems [10–12]. The present paper is applied to balance the dynamic imbalance response of rotating the composite hollow shaft by developing a working mathematical model.

2. Materials and methods

2. 1. Object of study

As illustrated in **Fig. 1**, the composite hollow circular cross-section shaft is made using HM Carbon/Epoxy composite hollow shafts when high strength and stiffness are required [13]. In comparison, hollow circular shafts are stronger per kg weight than solid circular shafts; also, the solid shaft has zero stress distribution at the end maximum at the outer surface, but the stress variation in hollow shafts is smaller [14, 15].



Fig. 1. Composite hollow shaft provided by rock west composites [16]

Table 1 displays the mechanical and geometric parameters of the composite hollow shaft material. The composite hollow shaft is made with three layers and the stacking sequence 0/45/45 since this stacking sequence allows for higher shear force to be applied to the shaft.

Table 1

Mechanical and geometric parameters of the composite hollow shaft

Property	Symbol	Value	Units
Young's modulus of elasticity	E	90	GPa
Poisson's ratio	ν	0.14	–
Shear modulus	G	4.6	GPa
Density	ρ	1600	Kg/m ³
Outer diameter	d_o	25	mm
Inner diameter	d_{in}	22.2	mm
Wall thickness	T	1.4	mm

In this study, the dynamic behaviour of a hollow shaft is represented using a simplified homogenized beam theory (SHBT) [17]. **Table 1** contains the values that are utilized to calculate the stiffness EI of the hollow shaft using the equations from [18].

2. 2. Modelling procedures

To eliminate the commonality imbalance mass of the rotors, a distinct dynamic balancing approach has been presented. These methods may be divided into two categories: influence coefficient balancing methods and modal balancing methods [19–21].

In this technique, the influence coefficient approach is a flexible rotor balancing procedure that works at various speeds. The flexible rotor was essential to compare in numerous planes, which relied on the number of critical speeds, in order to estimate a response matrix. The linear relationship between changes in the vector of response to change on applied to unbalance is determined in this method by defining the vibration response at one measurement point that is excited by a single unbalance in one of the balancing planes, which can be determined using a numerical method.

The influence coefficient technique can be quite costly since it requires several test runs with stops, restarts, and cooling down procedures. As shown in **Fig. 2**, a simple rotor system was implemented, and the influence coefficients are relationships between imbalance force $F_k = U_k \cdot \Omega^2$ as an input performed in one of the compensation plans, k , and output are for vibration response in measurement plane x_i at bearing sites. Where U_k denotes the applied test weight in the balancing plane k and Ω is a rotating frequency. The influence coefficient may then be calculated as follows:

$$\alpha_{ik(\Omega)} = \frac{x_i(\Omega)}{U_k} = \alpha_{ikRe} + j \cdot \alpha_{ikIm}$$

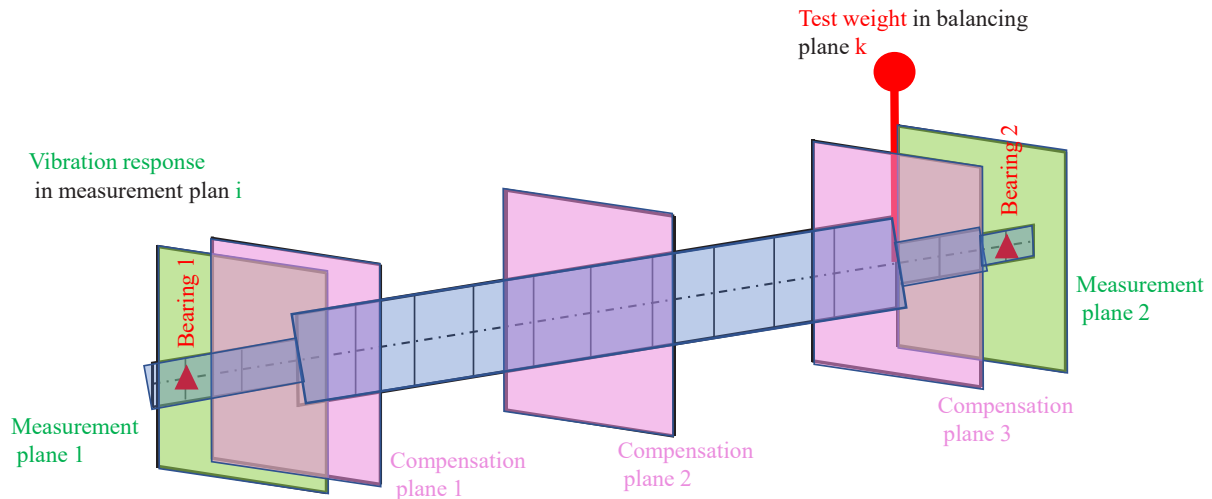


Fig. 2. Influence coefficient as a complex output/input relation [22]

The modal balancing method is a multi-plane flexible rotor balancing technique. It is a developed alternative to the influence-coefficient approach, however, the rotor dynamic characteristics require prior knowledge of the system. The excitations of the modes are balanced one by one in this manner, and then the concept of modal superposition is used of a particular number of a modal response, to balance a higher mode, a trial mass set with little influence on the preceding modes is utilized.

The following information to balance a ℓ_{th} mode of interest, the total imbalance mass distribution b_c on the rotor due to the initial unbalance, and any unbalance corrections applied:

$$u_\ell b_c = 0,$$

where u_ℓ is the ℓ_{th} mode shape and represents the eigenvector related to the ℓ_{th} eigenvalue. In addition, the total number of the unbalance mass correction of each mode of interest is:

$$b_{ci} = b_{c1} + b_{c2} + \dots,$$

and for some arbitrary (complex) scalars factor α_i and exists some sequence basis vectors $\mathbf{e}_1, \mathbf{e}_2, \dots$ then, the total unbalance mass correction is using $b_{ci} = \alpha_i \mathbf{e}_i$ for all i . The theoretical foundations of modal balancing are presented in-depth in the book 'Dynamics of rotating machines' [23, 24] and the rotodynamic response, such as model form and critical speed, may be numerically computed using the MATLAB software program. Although the modal balancing method usually requires prior knowledge of the system in order to correctly select balancing planes, it is simple to apply and the number of runs is reduced due to the use of trial mass set rather than individual mass by mass; additionally, due to the use of speed closer to critical speed, it has a high sensitivity to unbalance. The Unified Balancing Approach may be used to handle modal balancing issues and combine the benefits of the influence coefficients method with the modal balancing method. This research looks at the theoretical feasibility of balancing the imbalanced rotor response using a numerical simulation model. The MATLAB code is used to create a working mathematical model of the rotor-bearing system. The imbalanced rotor-bearing system finite element model is proposed. As illustrated in **Fig. 3**, the suggested finite element model is created by selecting 7 nodes on the rotor-bearing model to enhance simulation accuracy and increase the model's degree of freedom. The shaft is divided into 6 equal elements of $l_e = 0.15$ m in this model, and the first and seventh nodes are chosen to be the position of the bearings, which are represented as simple shaft supports. The anisotropic spherical roller bearing type (8-ball bearing on this work) is used, and the horizontal to vertical stiffness ratio is 0.46. The identical two disks are made of solid steel ($\rho = 7800$ kg/m³) and have a diameter of 150 mm and a thickness of 20 mm, with the matching nodes placed at nodes 3 and 5. The interior diameter d_i of the disk is considered to be the shaft's exterior diameter.

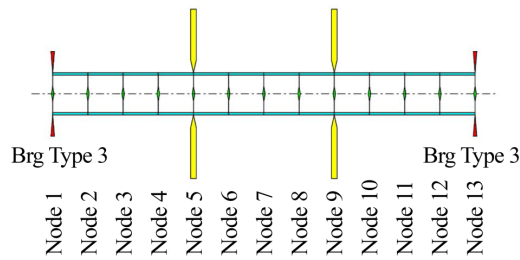


Fig. 3. The layout of the proposed model

3. Results and discussion

The rotor imbalance response before balancing is simulated and depicted in Fig. 4. Because of the mass unbalance, the vibration response pattern is seen, with a peak amplitude response of 10 mm at the first critical speed of 750 rpm, corresponding to node 5.

At the first critical speed, this rotor must be balanced using a single corrective mass at the balancing plane point at node 5, which reflects the highest vibration response amplitude at the first critical speed.

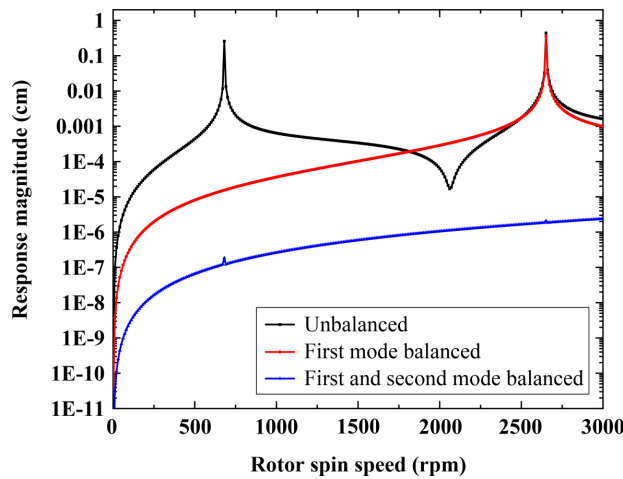


Fig. 4. Rotor spin speed at node 5

The N-plane modal balancing approach is used to balance the rotor at the first critical speed, hence at plane 5, a single imbalance correction mass of 200 g.m at 120 degrees is required to balance the rotor at the first critical frequency.

The amplitude response at the first critical speed is then determined, as illustrated in Fig. 4 after the corrective mass is introduced at plan 5 (Node 5). As indicated in Table 2, the maximum amplitude of the vibration corresponding to node 5 is 232 μm, which is much less than before the balancing around 0.1 cm.

Table 2

Comparison of vibration amplitude

Disk vibration status	Vibration amplitude at first critical speed (682 rpm)	Vibration amplitude at first critical speed (2658 rpm)
Before balancing	0.258 cm	1.85 cm
After balancing	1.1e-7 cm	1.8e-6

As can be seen in Fig. 5, the mass unbalances the unstable condition is observed at node 7 (which is the x-axis of the first disk) by demonstrating the response of the two unbalanced mass conditions model through operation speed of the rotor shaft, which is about 25 mm and 75 mm

at 1500 rpm and 3000 rpm, respectively. The maximum amplitude of the balancing spinning shaft, on the other hand, is greatly reduced to around 0.1 mm at 3000 rpm and 0.01 mm at 1500 rpm. The simulation results ranged from 0 to 200 seconds in 1-second increments.

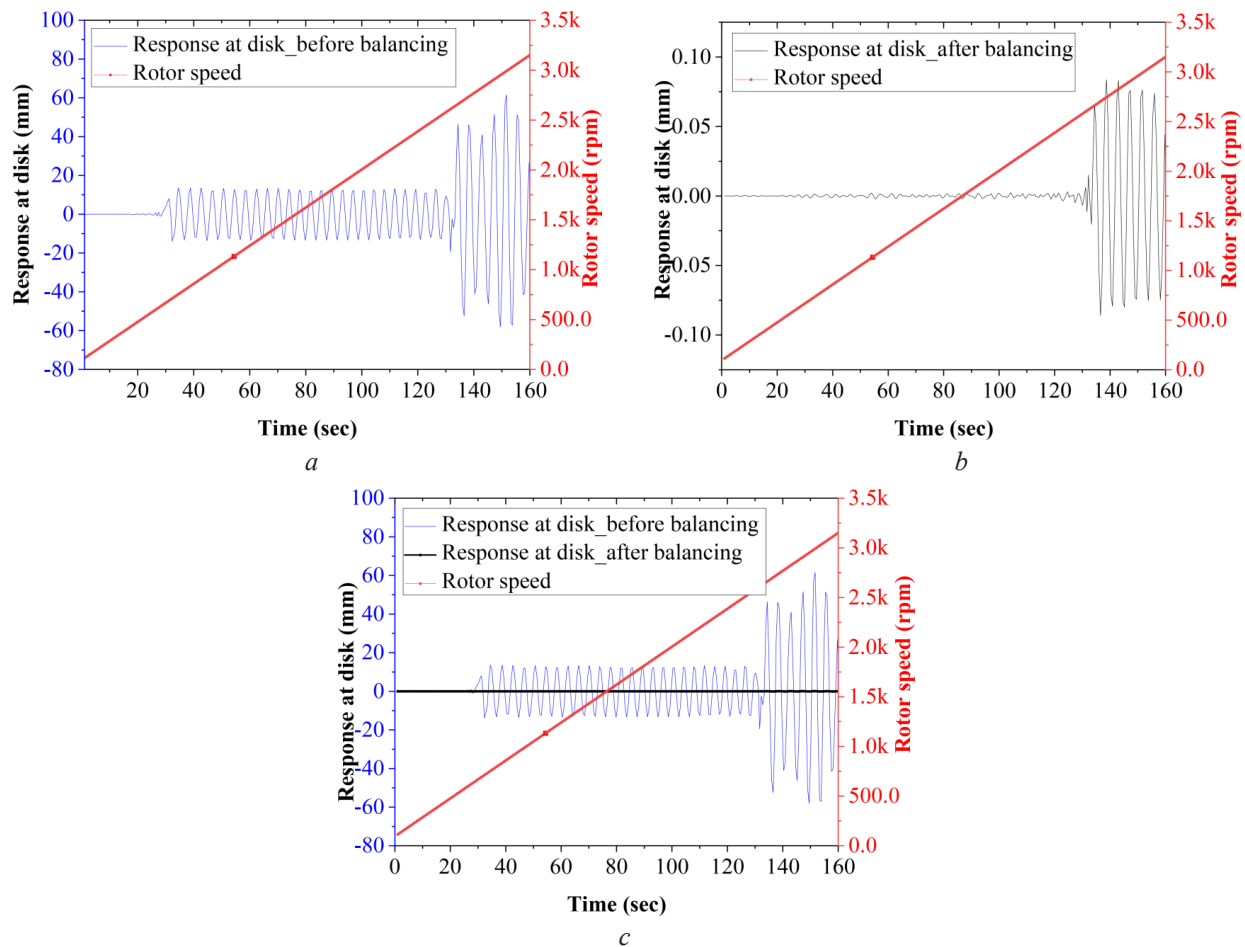


Fig. 5. Comparison of the disk vibration response of the considered model operation from 100 rpm to 4000 rpm: *a* – before balancing; *b* – after balancing; *c* – both of models before and after disk balancing

4. Conclusions

The current study validates the process for distributing imbalance in modelling balancing to balance the flexible hollow shaft with an unbalanced mass throughout the whole speed range of the shaft. The balance of the hollow shaft at the critical speed was observed in this manner, and the vibration amplitude was determined by adding extra mass at a specific angle.

Finally, the suggested approach was used to balance the hollow shaft, and the results were compared, including the first and second modes of the dynamic response to the unbalanced shaft, which brings a significant improvement in the vibration of the shaft at critical speed crossings.

References

- [1] Al-Falahat, A., Abu, Q., Alwashdeh, S. (2022). Economic feasibility of heating source conversion of the swimming pools. *Journal of Applied Engineering Science*, 20 (1), 230–238. doi: <https://doi.org/10.5937/jaes0-34474>
- [2] Lee, C.-W. (1993). *Vibration Analysis of Rotors*. Springer. doi: <https://doi.org/10.1007/978-94-015-8173-8>
- [3] Al-Falahat, A. M. (2021). Examination of the Dynamic Behaviour of the Composite Hollow Shafts Subject to Unbalance. *International Journal of Mechanical Engineering and Robotics Research*, 572–576. doi: <https://doi.org/10.18178/ijmerr.10.10.572-576>
- [4] Fedak, V., Zaskalicky, P., Gelvanič, Z. (2014). Analysis of Balancing of Unbalanced Rotors and Long Shafts using GUI MATLAB. *MATLAB Applications for the Practical Engineer*. doi: <https://doi.org/10.5772/58378>

- [5] Ahobal, N., Ajit prasad, S. L. (2019). Study of vibration characteristics of unbalanced overhanging rotor. IOP Conference Series: Materials Science and Engineering, 577 (1), 012140. doi: <https://doi.org/10.1088/1757-899x/577/1/012140>
- [6] Choudhury, T., Viitala, R., Kurvinen, E., Viitala, R., Sopanen, J. (2020). Unbalance Estimation for a Large Flexible Rotor Using Force and Displacement Minimization. Machines, 8 (3), 39. doi: <https://doi.org/10.3390/machines8030039>
- [7] Chawla, K. K. (2019). Composite Materials. Springer. doi: <https://doi.org/10.1007/978-3-030-28983-6>
- [8] Majewski, T., Szwedowicz, D., Melo, M. A. M. (2015). Self-balancing system of the disk on an elastic shaft. Journal of Sound and Vibration, 359, 2–20. doi: <https://doi.org/10.1016/j.jsv.2015.06.035>
- [9] Al-Falahat, A. M., Kardjilov, N., Khanh, T. V., Markötter, H., Boin, M., Woracek, R. et. al. (2019). Energy-selective neutron imaging by exploiting wavelength gradients of double crystal monochromators – Simulations and experiments. Nuclear Instruments and Methods in Physics Research Section A: Accelerators, Spectrometers, Detectors and Associated Equipment, 943, 162477. doi: <https://doi.org/10.1016/j.nima.2019.162477>
- [10] Al-Falahat, A. M., Qadourah, J. A., Alwashdeh, S. S., khater, R., Qatlama, Z., Alddibs, E., Noor, M. (2022). Energy performance and economics assessments of a photovoltaic-heat pump system. Results in Engineering, 13, 100324. doi: <https://doi.org/10.1016/j.rineng.2021.100324>
- [11] Abu Qadourah, J., Al-Falahat, A. M., Alwashdeh, S. S., Nytsch-Geusen, C. (2022). Improving the energy performance of the typical multi-family buildings in Amman, Jordan. City, Territory and Architecture, 9 (1). doi: <https://doi.org/10.1186/s40410-022-00151-8>
- [12] Abu qadourah Jenan, Al-Falahat, A., Alwashdeh, S. (2022). Investigate the carbon footprints of three intermediate flooring systems: cross-laminated timber, solid concrete, and hollow-core precast concrete. Journal of Applied Engineering Science, 1–6. doi: <https://doi.org/10.5937/jaes0-32783>
- [13] Bodake, P. M., Aher, V. S. (2018). Design and Analysis of Composite Drive Shaft. International Journal for Research in Applied Science and Engineering Technology, 6 (5), 1570–1576. doi: <https://doi.org/10.22214/ijraset.2018.5254>
- [14] Yeswanth, I. V. S., Andrews, A. A. E. (2017). Parametric optimization of composite drive shaft using ansys workbench 14.0. International Journal of Mechanical Engineering and Technology (IJMET), 8 (5). Available at: https://www.academia.edu/36839862/PARAMETRIC_OPTIMIZATION_OF_COMPOSITE_DRIVE_SHAFT_USING_ANSYS_WORKBENCH_14_0
- [15] Alwashdeh, S. S., Alsaraireh, M. F., Saraireh, A. M., Markötter, H., Kardjilov, N. (2018). In-situ investigation of water distribution in polymer electrolyte membrane fuel cells using high-resolution neutron tomography with 6.5 μm pixel size. AIMS Energy, 6 (4), 607–614. doi: <https://doi.org/10.3934/energy.2018.4.607>
- [16] Rock West Composites. Available at: <https://www.rockwestcomposites.com/>
- [17] Kennedy, G. J., Martins, J. R. R. A. (2012). A homogenization-based theory for anisotropic beams with accurate through-section stress and strain prediction. International Journal of Solids and Structures, 49 (1), 54–72. doi: <https://doi.org/10.1016/j.ijsolstr.2011.09.012>
- [18] Sino, R., Baranger, T. N., Chatelet, E., Jacquet, G. (2008). Dynamic analysis of a rotating composite shaft. Composites Science and Technology, 68 (2), 337–345. doi: <https://doi.org/10.1016/j.compscitech.2007.06.019>
- [19] Li, G., Lin, Z., Allaire, P. E. (2008). Robust Optimal Balancing of High-Speed Machinery Using Convex Optimization. Journal of Vibration and Acoustics, 130 (3). doi: <https://doi.org/10.1115/1.2890405>
- [20] Quartarone, C., Beqari, J., Detoni, J. G., Cometti, F., Emelli, E. (2019). Balancing of Turbomolecular Pumps: Modal Balancing Approach and Experimental Results. Proceedings of the 10th International Conference on Rotor Dynamics – IFToMM, 119–128. doi: https://doi.org/10.1007/978-3-319-99272-3_9
- [21] Alwashdeh, S. S., Ammari, H., Madanat, M. A., Al-Falahat, A. M. (2022). The Effect of Heat Exchanger Design on Heat transfer Rate and Temperature Distribution. Emerging Science Journal, 6 (1), 128–137. doi: <https://doi.org/10.28991/esj-2022-06-01-010>
- [22] Nordmann, R., Knopf, E., Abrate, B. (2019). Numerical Analysis of Influence Coefficients for On-Site Balancing of Flexible Rotors. Proceedings of the 10th International Conference on Rotor Dynamics – IFToMM, 157–172. doi: https://doi.org/10.1007/978-3-319-99272-3_12
- [23] Friswell, M. I., Penny, J. E. T., Garvey, S. D., Lees, A. W. (2010). Dynamics of Rotating Machines. Cambridge University Press. doi: <https://doi.org/10.1017/cbo9780511780509>
- [24] Norfield, D. (2005). Practical balancing of rotating machinery. Elsevier. doi: <https://doi.org/10.1016/b978-1-85617-465-7.x5000-1>

Received date 16.06.2021

Accepted date 17.03.2022

Published date 31.03.2022

© The Author(s) 2022

This is an open access article
under the Creative Commons CC BY license

How to cite: Al-Falahat, A. M. (2022). Implementation of the dynamic balancing approach of a rotating composite hollow shaft. EUREKA: Physics and Engineering, 2, 68–73. doi: <https://doi.org/10.21303/2461-4262.2022.002336>